American Mineralogist, Volume 76, pages 1502–1509, 1991

A structural investigation of oxidation effects in air-heated grunerite

Michael W. Phillips
Department of Geology, The University of Toledo, Toledo, Ohio 43606, U.S.A.
Robert K. Popp
Department of Geology, Texas A&M University, College Station, Texas 77843, U.S.A.
Celia A. Clowe
Department of Geological Sciences, Virginia Polytechnic Institute and State University, Blacksburg, Virginia 24061, U.S.A.

Abstract

Crystal structure refinements have been performed on four grunerite crystals in order to compare oxidation effects in the grunerite structure with those reported for calcic and alkali amphiboles. The crystals examined are natural grunerite (NAT) and samples that were air heated at 700 °C, 1 atm for durations of 30 min (30M) and 2 h (2HR-A, 2HR-B).

The initial stages of oxidation in grunerite consist of both dehydrogenation and, unlike calcic and alkali amphiboles, an "oxygenation" process that involves structural decomposition. SEM photographs of the oxidized grunerite samples reveal that decomposition products formed both as irregular subparallel ridges roughly perpendicular to the axis of elongation of the grunerite crystals and as small subhedral prismatic crystals along heating-induced cleavage traces parallel to the axis of elongation. The decomposition products are greatly enriched in Fe and depleted in Mg and Si relative to the grunerite, and the oxidized samples are slightly magnetic, suggesting that they are, at least in part, magnetite.

Site-refinement data suggest that Fe is preferentially lost from M4 with oxidation, resulting in about 7% vacant M4 sites in the crystals heated for 2 h. There also appear to be smaller amounts of Fe loss from M3 and M2 but not M1.

These results agree with earlier investigations that indicate the grunerite structure is less able to accommodate the oxy-amphibole component than are the calcic and alkali amphibole structures.

Introduction

Barnes (1930) reported that oxidation in hornblende and actinolite proceeds by a dehydrogenation reaction. This suggests that for each Fe^{2+} oxidized to Fe^{3+}, there is a loss of one H atom from an OH group at an O3 site. Dehydrogenation is also believed to be the sole initial oxidation mechanism in alkali amphiboles, but not in grunerite (see Hawthorne, 1983).

Hodgson et al. (1965) found that heating fibrous grunerite ("amosite") in air in the range between about 500 and 800 °C produced "oxy-grunerite," indicating dehydrogenation. However, they discovered that the Fe^{2+} content in these samples decreased by a much greater amount than would be expected from oxidation-dehydrogenation alone. Furthermore, they observed a slight weight increase in the samples that also suggests dehydrogenation is not the only oxidation mechanism operating in grunerite. This concurrent oxidation process in grunerite was termed "oxygenation" by Hodgson et al. (1965), although no precise oxygenation reaction was proposed. These findings were confirmed in investigations by Addison and Sharp (1968) and Rouxhet et al. (1972); however, the exact nature of the oxygenation mechanism could not be determined.

Phillips et al. (1988) calculated bond strengths for a variety of amphiboles with appreciable oxy-amphibole content and found that dehydrogenation led to a local charge imbalance at the O3 site. They concluded that the structural stability (or metastability) of an amphibole undergoing oxidation depends upon the extent to which minor structural adjustments are able to offset the local charge imbalance arising at O3 as a result of dehydrogenation. These adjustments include: (1) compensational shortening of O3 bonds to M3 and particularly M1, (2) ordering of Fe^{3+} produced by oxidation at M1 or M3 rather than at M2, (3) reordering of trivalent cations from M2 to M1 or M3, (4) interaction of the A-site cation with O at O3, (5) and, at least in air-heated samples, some transfer of Na (or Ca) from M4 to the A site if A-site vacancies exist. Phillips et al. (1988) pointed out that, whereas all five compensational mechanisms may be operative in calcic or alkali amphiboles, only the first two are possible in grunerite. They suggested that this difference may account for the different oxidation behavior observed in grunerite.

The present study was undertaken to examine the actual extent of structural adjustments in oxidized grunerite and to investigate further the oxygenation reaction observed by Hodgson et al. (1965). Crystal-structure refine-

0003–004X/91/0910–1502$02.00

ment data are presented for natural grunerite (NAT) and for samples that were air heated at 700 °C for durations of 30 min (30M) and 2 h (2HR-A, 2HR-B). Heating experiment details are given by Clowe et al. (1988).

Experimental procedure

Sample description

The natural grunerite investigated by Clowe et al. (1988) is from the same general sample (Klein, 1964, sample 1) that was used for crystal-structure refinement by Finger (1969). Using the single-dissolution wet chemical method of Fritz and Popp (1985), Clowe et al. (1988) found no Fe^{3+} in the natural sample (NAT); however, the ferric/ferrous ratios, $R = Fe^{3+}/(Fe^{2+} + Fe^{3+})$, increased to $R = 0.16(2)$ and $R = 0.27(2)$ in the samples heated for 30 min (30M) and 2 h (2HR-A, 2HR-B), respectively.

Electron-microprobe analysis of the natural sample by Clowe et al. (1988) indicates small amounts of Mn and Ca present (0.09 and 0.06 atoms per formula unit, respectively) which is in good agreement with the analysis of Klein (1964) that shows 0.05 Mn and 0.06 Ca per formula unit. Clowe et al. (1988) also report small amounts of Al (0.10), Na (0.10), Ti (0.01), and Cl (0.01). Clowe et al. (1988) also analyzed the 30-min experimental product with similar results, except that the Na content was lower (0.02). There is a major discrepancy between F contents reported by Klein (0.51) and by Clowe et al. (0.09). It is not clear whether this difference represents analytical error or a high degree of local variability of F content in the Klein (1964) grunerite. For purposes of crystal structure refinement, the initial chemical composition was simplified to $Fe_6MgSi_8O_{22}(OH)_2$.

Rapid oxidation induced by air heating has an adverse effect on the crystal quality of tschermakitic hornblende (Phillips et al., 1989). This was even more evident in grunerite, particularly the sample air heated for 2 h. A number of crystals were examined on the CAD4 diffractometer before one was found that yielded 25 orientation reflections that could be properly indexed. Oscillation photographs of this crystal (2HR-A) revealed a number of reflections that appeared slightly "fuzzy," which is consistent with the peak broadening observed in powder patterns and CAD4 peak profiles. Because structure refinements of the data set for this crystal (2HR-A) yielded relatively large estimated standard deviation and R values, a second crystal was selected (again, with some difficulty) for intensity data collection. Based on ω-θ plots of several reflections, an ω scan was used to obtain intensity data for this crystal (2HR-B). This refinement yielded values and errors similar to those of crystal 2HR-A with the notable exception of thermal parameters. The isotropic equivalent temperature factors are much higher for the refinement of crystal 2HR-B than for 2HR-A. Although the reason for this discrepancy is not clear, given the extent of damage that these crystals experienced during heating (see Fig. 1), it seems reasonable to suspect the cause was crystal quality rather than data measurement parameters.

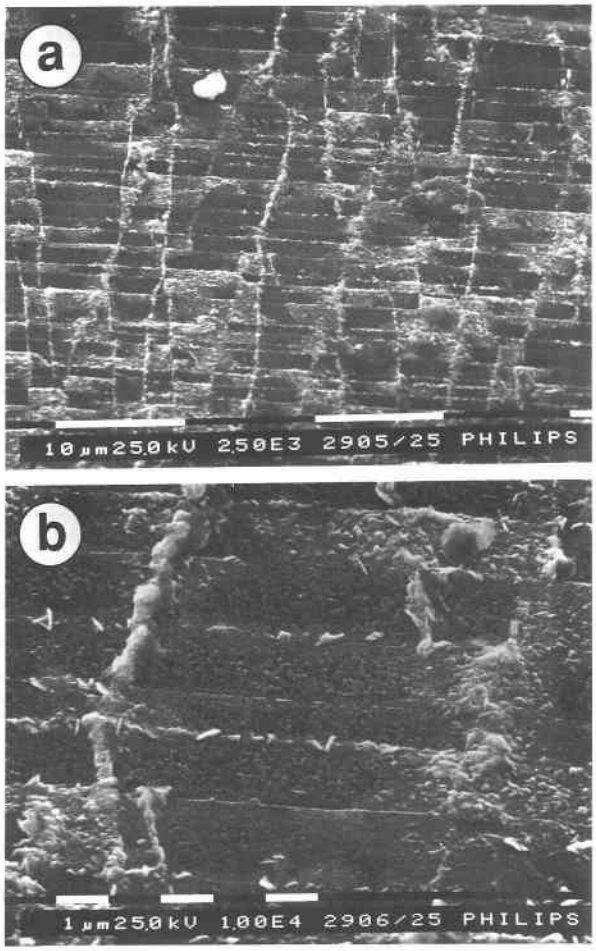

Fig. 1. Secondary electron images of grunerite grains air heated at 700 °C for 2 h. The vertical ridges were visible optically and are greatly enriched in Fe relative to the grunerite. The horizontal features appear to be incipient cleavage traces parallel to the elongate axis of the crystal along which small subhedral prismatic crystals have formed. (**a**) Lower magnification; (**b**) central portion of **a** at higher magnification. Photographs were provided by Bob Anderhalt, Philips Electronic Instruments, Mahwah, New Jersey.

Intensity data measurement and structure refinement

Intensities of the type hkl, $k \geq 0$ were measured using a variable scan speed (1–7°/min) on an automated Enraf-Nonius CAD4 diffractometer utilizing graphite-monochromatized Mo$K\alpha$ radiation ($\lambda = 0.71073$ Å). An attenuator was automatically inserted for intense reflections. Background counts were determined by scanning 25% above and below the actual peak scan width. Additional data collection and refinement parameters are given in Table 1 along with the unit-cell parameters determined by least-squares refinement of 25 measurements of diffractometer-centered reflections between 27 and 33° 2θ.

Data were corrected for background and Lorentz-polarization effects and for absorption using a series of ψ scans (North et al., 1968). In the final stages of refine-

Table 1. Data measurement and refinement parameters and unit-cell dimensions

	NAT	30M	2HR-A	2HR-B
Crystal size (mm)	0.16 × 0.06 × 0.04	0.18 × 0.06 × 0.04	0.25 × 0.11 × 0.04	0.23 × 0.10 × 0.04
Max. sin θ/λ	0.8064	0.8066	0.8058	0.8071
Scan speed (ω)	1–7°/min	1–7°/min	1–7°/min	1–7°/min
Scan width (°)	0.8 + 0.34 tan θ	0.9 + 0.34 tan θ	1.1 + 0.34 tan θ	1.2 + 0.34 tan θ
Total reflections (excluding stds.)	4149	4124	4078	4057
Unique reflections	2083	2071	2050	2050
Averaging agreement (on F) for accepted reflections	1.7%	1.7%	3.6%	3.2%
Accepted reflections	1492	1490	1167	1192
Extinction coefficient	1.47(2) × 10^{-6}	2.1(2) × 10^{-7}	—	2.1(4) × 10^{-7}
Final R	2.0%	2.3%	4.6%	4.0%
Final R_w	2.0%	2.4%	4.9%	4.1%
		Unit-cell dimensions		
a (Å)	9.570(2)	9.547(2)	9.526(2)	9.508(4)
b (Å)	18.397(3)	18.355(4)	18.301(3)	18.248(8)
c (Å)	5.342(2)	5.329(2)	5.319(2)	5.313(1)
β (°)	101.94(3)	101.95(2)	101.92(2)	101.85(3)
V (Å^3)	920.2(6)	913.6(7)	907.3(7)	902.2(10)

Note: Estimated standard deviations are given in parentheses and refer to the last decimal place in this and in subsequent tables.

ment, the absorption correction was slightly improved using the empirical method of Walker and Stuart (1983). Reflections with $I < 3\sigma$ (I), as determined by counting statistics, were considered unobserved. Equivalent reflections were averaged, and reflections of the type $|I - I_{avg}| > 5\sigma$ (I) were rejected.

Scattering factors for neutral atoms were taken from the *International Tables for X-ray Crystallography* (1974). All atoms except H were corrected for anomalous dispersion effects (Ibers and Hamilton, 1964). An isotropic extinction coefficient (Zachariasen, 1963, 1967) was included as a variable in all refinements except for 2HR-A where no correction was indicated. Calculations were performed on a VAX11/750 using the SDP/VAX program package (Frenz, 1978). Initial positional parameters were taken from Finger (1969), and unit weights were used for all refinements. All site refinements of Fe and Mg constrained only the total occupancy (assumed to be 1.0) of each M site. All structures were refined in space group $C2/m$.

After initial convergence with isotropic temperature factors, H positions were located from difference-Fourier maps calculated for the x-z section coincident with the mirror plane. In addition to the H peak, a number of smaller features were observed in the vicinity of O3, possibly because any F present may be slightly shifted in the x-z plane relative to OH. Perhaps for this reason, attempts to refine H occupancies following the procedure described by Phillips et al. (1989) for oxidized tschermakitic hornblende proved unsuccessful. Because oxidation of grunerite proceeds by "oxygenation" and dehydrogenation concurrently (Hodgson et al., 1965), it was also impossible to estimate the OH content of the oxidized samples from changes in the Fe^{3+}/Fe^{2+} ratios. Therefore, in subsequent refinements the H occupancies were arbitrarily fixed at a value of 1.0 for all four structures.

In the final refinements, the scale factor, absorption coefficient, all positional parameters, anisotropic temperature factors (except for H where B was arbitrarily fixed at 1.0), and the constrained Fe-Mg occupancies of M1, M2, M3, and M4 were allowed to vary simultaneously. The final atomic parameters (Table 2), interatomic distances and angles (Table 3), and site-occupancy data (Table 4) were taken from these refinements. Additional thermal parameters (Table 5) and the list of observed and calculated structure factors (Table 6) are available on microfiche.[1]

Results

Scanning electron microscopy (SEM)

Examination of the oxidized samples with a polarizing microscope indicated that some crystals have small irregular linear features roughly perpendicular to the elongate axis (presumably the **c** crystallographic axis) of the crystal. These features are difficult to observe optically because absorption increases dramatically with oxidation and even most small grains do not transmit light sufficiently well for these features to be observed.

A preliminary SEM examination of both the 30-min and 2-h air-heated samples indicated that these features are irregular masses of a secondary phase that form as ridges on the surface of the grunerite and are present on all air-heated crystals. These appear as the vertical features in Figure 1. A second linear set, parallel to the elongated axis of the crystal (the horizontal features in Fig. 1), that is more regular and more closely spaced than the vertical set of Figure 1 was also observed on most oxidized crystals. This second set is formed by small subhedral crystals distributed along what appear to be incip-

[1] A copy of Tables 5 and 6 may be ordered as Document AM-91-472 from the Business Office, Mineralogical Society of America, 1130 Seventeenth Street NW, Suite 330, Washington, DC 20036, U.S.A. Please remit $5.00 in advance for the microfiche.

TABLE 2. Final atomic parameters and B_{eqv}

Atom	structure	x	y	z	B_{eqv}
T1	NAT	0.28639(5)	0.08356(2)	0.27028(9)	0.454(6)
	30M	0.28721(6)	0.08350(3)	0.27099(11)	0.516(8)
	2HR-A	0.28835(16)	0.08351(8)	0.27188(27)	0.59(2)
	2HR-B	0.28905(13)	0.08361(7)	0.27292(23)	1.25(2)
T2	NAT	0.29900(5)	0.16679(3)	0.77699(9)	0.487(6)
	30M	0.29908(6)	0.16691(3)	0.77755(11)	0.542(8)
	2HR-A	0.29916(16)	0.16709(8)	0.77814(27)	0.57(2)
	2HR-B	0.29909(13)	0.16710(7)	0.77806(23)	1.27(2)
M1	NAT	0	0.08788(2)	½	0.560(5)
	30M	0	0.08730(3)	½	0.632(7)
	2HR-A	0	0.08569(7)	½	0.77(2)
	2HR-B	0	0.08480(6)	½	1.47(2)
M2	NAT	0	0.17941(2)	0	0.518(6)
	30M	0	0.17945(3)	0	0.580(7)
	2HR-A	0	0.17975(7)	0	0.60(2)
	2HR-B	0	0.17964(6)	0	1.35(2)
M3	NAT	0	0	0	0.520(7)
	30M	0	0	0	0.576(9)
	2HR-A	0	0	0	0.59(2)
	2HR-B	0	0	0	1.32(2)
M4	NAT	0	0.25740(2)	½	0.801(6)
	30M	0	0.25748(3)	½	0.825(7)
	2HR-A	0	0.25766(7)	½	0.86(2)
	2HR-B	0	0.25775(6)	½	1.57(2)
O1	NAT	0.1137(1)	0.0884(1)	0.2055(2)	0.60(2)
	30M	0.1144(2)	0.0884(1)	0.2069(3)	0.68(2)
	2HR-A	0.1149(4)	0.0889(2)	0.2076(7)	0.75(6)
	2HR-B	0.1157(3)	0.0887(2)	0.2104(6)	1.42(5)
O2	NAT	0.1262(1)	0.1737(1)	0.7153(2)	0.69(2)
	30M	0.1259(2)	0.1733(1)	0.7155(3)	0.78(2)
	2HR-A	0.1248(4)	0.1720(2)	0.7144(7)	0.83(6)
	2HR-B	0.1243(3)	0.1714(2)	0.7143(6)	1.66(6)
O3	NAT	0.1144(2)	0	0.7047(4)	0.84(3)
	30M	0.1138(3)	0	0-.7053(5)	0.98(4)
	2HR-A	0.1118(7)	0	0.7046(12)	1.10(10)
	2HR-B	0.1106(6)	0	0.7047(10)	1.82(9)
O4	NAT	0.3840(1)	0.2418(1)	0.7680(3)	0.84(2)
	30M	0.3832(2)	0.2422(1)	0.7686(3)	0.99(2)
	2HR-A	0.3819(5)	0.2434(2)	0.7700(8)	1.14(7)
	2HR-B	0.3813(4)	0.2435(2)	0.7705(7)	1.92(6)
O5	NAT	0.3497(1)	0.1284(1)	0.0567(3)	0.91(2)
	30M	0.3501(2)	0.1287(1)	0.0579(3)	0.93(2)
	2HR-A	0.3510(4)	0.1290(2)	0.0603(8)	0.97(6)
	2HR-B	0.3514(4)	0.1290(2)	0.0589(6)	1.68(6)
O6	NAT	0.3479(1)	0.1175(1)	0.5520(3)	1.04(2)
	30M	0.3490(2)	0.1179(1)	0.5529(3)	1.13(3)
	2HR-A	0.3503(5)	0.1184(3)	0.5542(8)	1.19(7)
	2HR-B	0.3512(4)	0.1194(2)	0.5542(7)	1.91(6)
O7	NAT	0.3389(2)	0	0.2688(4)	0.98(3)
	30M	0.3396(3)	0	0.2694(5)	0.96(4)
	2HR-A	0.3410(6)	0	0.2714(12)	0.99(9)
	2HR-B	0.3424(5)	0	0.2728(10)	1.69(8)
H	NAT	0.312(4)	½	0.263(7)	1.0*
	30M	0.316(5)	½	0.270(9)	1.0*
	2HR-A	0.320(12)	½	0.277(21)	1.0*
	2HR-B	0.320(8)	½	0.266(14)	1.0*

* For H the isotropic temperature factors were arbitrarily fixed at B = 1.0.

TABLE 3. Selected interatomic distances (Å) and angles (°)

	NAT	30M	2HR-A	2HR-B
T(1)-O(1)	1.619(1)	1.617(2)	1.619(4)	1.616(3)
-O(5)	1.623(2)	1.619(2)	1.610(5)	1.614(4)
-O(6)	1.623(1)	1.624(2)	1.626(4)	1.627(4)
-O(7)	1.618(1)	1.613(1)	1.609(2)	1.608(2)
mean	1.621	1.618	1.616	1.616
O(1)-T(1)-O(5)	109.56(7)	109.52(8)	109.3(2)	109.4(2)
-O(6)	109.60(7)	109.45(9)	109.3(2)	109.2(2)
-O(7)	110.79(8)	110.84(10)	111.2(3)	111.3(2)
O(5)-T(1)-O(6)	109.89(7)	109.48(9)	109.0(2)	108.9(2)
-O(7)	108.54(10)	108.81(12)	109.2(3)	109.0(3)
O(6)-T(1)-O(7)	108.44(9)	108.72(11)	108.7(3)	109.1(2)
mean	109.47	109.47	109.5	109.5
T(2)O(2)	1.623(1)	1.622(2)	1.627(4)	1.628(3)
-O(4)	1.607(1)	1.604(2)	1.608(5)	1.602(4)
-O(5)	1.633(1)	1.631(2)	1.636(4)	1.629(4)
-O(6)	1.649(2)	1.645(2)	1.640(5)	1.630(4)
mean	1.628	1.626	1.628	1.622
O(2)-T(2)-O(4)	115.32(7)	115.29(9)	115.6(2)	115.8(2)
-O(5)	108.47(7)	108.46(9)	108.4(2)	108.5(2)
-O(6)	109.00(7)	109.12(8)	108.8(2)	108.9(2)
O(4)-T(2)-O(5)	110.02(7)	109.98(9)	109.8(2)	109.6(2)
-O(6)	103.24(8)	103.14(10)	103.4(3)	102.9(2)
O(5)-T(2)-O(6)	110.70(7)	110.77(9)	110.9(2)	111.1(2)
mean	109.46	109.46	109.5	109.5
M(1)-O(1) ×2	2.090(1)	2.083(2)	2.080(4)	2.068(4)
-O(2) ×2	2.167(1)	2.164(2)	2.156(4)	2.153(3)
-O(3) ×2	2.124(1)	2.110(1)	2.074(4)	2.052(3)
mean	2.127	2.119	2.103	2.091
M(2)-O(1) ×2	2.168(1)	2.168(2)	2.164(4)	2.171(3)
-O(2) ×2	2.132(1)	2.124(2)	2.119(4)	2.112(4)
-O(4) ×2	2.074(1)	2.065(2)	2.043(4)	2.041(4)
mean	2.125	2.119	2.109	2.108
M(3)-O(1) ×4	2.130(1)	2.132(2)	2.136(4)	2.138(3)
-O(3) ×2	2.098(2)	2.087(3)	2.072(7)	2.060(6)
mean	2.119	2.117	2.115	2.112
M(4)-O(2) ×2	2.140(1)	2.140(2)	2.148(4)	2.151(3)
-O(4) ×2	1.985(2)	1.988(2)	1.999(5)	2.002(4)
-O(5) ×2	3.269(1)	3.251(2)	3.228(4)	3.225(3)
-O(6) ×2	2.768(2)	2.749(2)	2.726(5)	2.697(4)
mean VI	2.298	2.292	2.291	2.283
mean VIII	2.541	2.532	2.525	2.519
H-O(3)	0.69(4)	0.66(5)	0.64(11)	0.64(7)
T(1)-O(5)-T(2)	141.23(9)	141.16(11)	141.0(3)	141.0(2)
T(1)-O(6)-T(2)	141.63(9)	141.41(11)	141.1(3)	141.0(2)
T(1)-O(7)-T(1)	143.71(14)	143.74(17)	143.6(4)	143.2(4)
O(5)-O(6)-O(5)	171.36(8)	171.50(10)	171.7(2)	172.5(2)
O(7)-O(7)-O(7)	58.73(5)	58.67(6)	58.6(2)	58.5(1)

ient cleavage traces. Neither of these two sets was observed on crystals of the natural grunerite.

The 2-h sample was sent to Robert Anderhalt, Philips Electronic Instruments, Mahwah, New Jersey, for further analysis by a Philips-525M SEM equipped with an EDAX 990 energy dispersive system (EDS). X-ray maps acquired simultaneously for Si, Fe, Mg, Al, Mn, and Ca over a period of 4 h show that both linear sets are enriched in Fe and depleted in Si and Mg relative to the grunerite. The X-ray signal maps for Al, Mn, and Ca are not as well defined because of their low concentrations. However, these maps indicate a uniform distribution of the respective elements with no areas of concentration or depletion, which suggests that these elements remain in the grunerite during oxidation-dehydrogenation.

Crystal structure refinement

M site occupancies. Site refinements were performed considering each M site to be fully occupied by only Fe and Mg. The refined Fe populations are given in Table 4; however, because the air-heated crystals experienced slight decomposition as evidenced by the presence of the secondary phase(s), it is more instructive to consider occupancy in terms of electrons per site rather than atoms per site. The number of electrons per site and the estimated errors were calculated from the respective Fe-Mg occupancies and are also shown in Table 4.

Examination of Table 4 reveals that as oxidation proceeded, the total number of M electrons per formula unit

TABLE 4. M-site occupancies

Site	NAT	30M	2HR-A	2HR-B
	Apparent Fe occupancies by site refinement			
M1	0.863(2)	0.856(3)	0.868(6)	0.865(5)
M2	0.779(2)	0.785(3)	0.743(6)	0.746(5)
M3	0.881(3)	0.852(4)	0.852(9)	0.864(7)
M4	0.951(2)	0.904(3)	0.834(6)	0.821(5)
Total pfu	6.07(1)	5.94(1)	5.74(2)	5.73(2)
	Electrons per site			
Site	NAT	30M	2HR-A	2HR-B
M1	24.08(3)	23.98(4)	24.15(9)	24.11(7)
M2	22.91(3)	22.99(4)	22.40(9)	22.44(7)
M3	24.33(4)	23.93(6)	23.93(13)	24.10(10)
M4	25.31(3)	24.66(4)	23.68(9)	23.49(7)
Total pfu	168.9(1)	167.2(2)	164.4(3)	164.2(3)

Note: Each site was constrained to full occupancy by Fe + Mg. Electrons/site = (Fe/site) × 26 + (1 − Fe/site) × 12.

TABLE 7. M-site occupancy changes with oxidation

Site	30M	2HR-A	2HR-B
	Changes in electrons/site relative to natural grunerite		
M1	0.10(5)	−0.07(9)	−0.03(8)
M2	−0.08(5)	0.51(9)	0.47(8)
M3	0.40(7)	0.40(14)	0.23(11)
M4	0.65(5)	1.63(9)	1.82(8)
	Number of vacancies created per site		
Site	30M	2HR-A	2HR-B
M1	0.004(2)	−0.003(3)	−0.001(3)
M2	−0.003(2)	0.020(3)	0.018(3)
M3	0.015(3)	0.015(5)	0.009(4)
M4	0.025(2)	0.063(3)	0.070(3)

Note: Changes = site (natural grunerite) − site (oxidized grunerite). Vacancies are assumed to arise from loss of Fe.

decreased from 168.9 (NAT) to 167.2 (30M) to 164.4 (2HR-A) or 164.2 (2HR-B). This indicates that some cations were lost from the M sites during oxidation. Because the EDS analysis indicates no Mg present in the secondary material, it is reasonable to assume that this cation loss represents Fe.

If there was little or no reordering of Fe-Mg among the M sites during oxidation and if all starting materials were homogeneous with respect to Fe-Mg content, then it is possible to examine the loss of cations from the individual M sites by comparing individual site occupancies in the oxidized structures with those in the natural grunerite (NAT). Electron microprobe analyses were performed prior to the heating experiments of Clowe et al. (1988) to insure that all materials chosen, including this grunerite sample, were homogeneous; hence, the latter assumption should be valid. Phillips et al. (1988, 1989) found significant reordering of trivalent cations originally residing at M2 in a tschermakitic hornblende heated under identical conditions for 30 min. They describe this reordering as an attempt by the structure to compensate for the loss of bond strength at O3 that accompanies oxidation-dehydrogenation. Unlike calcic or alkali amphiboles, natural grunerite contains few trivalent cations; therefore, there is no reason to suspect cation reordering in these structures for purposes of maintaining charge balance at O3. Still, Schurmann and Hafner (1971) and Ghose and Weidner (1972) found that the degree of Fe-Mg order in cummingtonite does depend in part on the temperature of equilibration. However, these grunerite samples contain much less Mg than the cummingtonite, and the duration of the heating experiments was much shorter for the grunerite than for the cummingtonite. Given these differences, it is not clear whether reordering should be expected in these grunerite samples. The occupancy data in Table 4 provide the strongest arguments against reordering in these structures. There are no significant variations among the electron occupancies of M1 for all four structures or among the occupancies of M3 for the three air-heated structures. This can only mean that in these cases either (1) no Fe-Mg exchange occurred at these sites during heating or (2) some Fe was lost from these sites; however, the electron occupancies happened to remain constant because every cation vacancy created at a particular site was also fortuitously accompanied by the substitution of 1.86 Fe for 1.86 Mg, on average, at that site. Given the improbable nature of such a coupled substitution, it appears likely that no appreciable reordering occurred at these sites during heating. Because no detectable cation vacancies are present in the untreated structure (NAT), the Fe distribution (Table 4) should represent true occupancies. Contrarily, the Fe values for the air-heated structures are only apparent occupancies because they were determined based on full M-site occupancy, which is clearly not the case given the decrease in the total M-site electrons per formula unit (Table 4). The Fe distribution in the NAT structure follows the site preference expected for iron magnesium manganese amphiboles, namely, M4 ≫ M3 ≥ M1 > M2 (Hawthorne, 1983). In crystals 2HR-A and 2HR-B, the apparent preference is M1 ≥ M3 > M4 > M2. Rather than assume that the anomalous Fe distribution observed in the structures heated for 2 h is real and represents substantial reordering of Fe-Mg, it seems more reasonable to consider it as only an artifact arising from the presence of cation vacancies at M4. In summary, it appears that Fe-Mg reordering was negligible in these structures and that the changes in the occupancies reported in Table 4 can be attributed to the presence of cation vacancies.

Using the electron site occupancies given in Table 4, changes that occurred during oxidation were estimated by subtracting the value for each M site in the oxidized structures from the respective site occupancy in the natural structure (see Table 7). Dividing these electron differences by 26 (the atomic number of Fe) gives an estimate of the number of cation vacancies in each individual site in the oxidized structures.

These values (Table 7) suggest that the majority of cations lost are from M4; specifically, it appears there are about 3% vacancies at M4 in the 30-min sample and about 6 or 7% in the 2-h samples. There also appears to be about 2% cation loss from M2 in the 2-h samples but not in 30-min samples. There may be a slight loss from

M3 as well. However, within the range studied, this apparent loss does not increase with increasing oxidation. These cation losses almost certainly represent the initial stages of oxidation-induced decomposition. Although speculation as to the structural mechanisms involved in decomposition beyond the oxidation range of these samples is not warranted, it is worth noting that vacancies at M4 and M2 represent the breaking of major bonds responsible for cross linking the basic I-beam modules of the structure (Papike and Ross, 1970).

The behavior of Ca. In calcic or sodic-calcic amphiboles, any small amounts of Fe or Mn on M4 order into a distinct M4′ site rather than in the principal M4 site occupied by Ca and Na (Bocchio et al., 1978). It appears that the converse is true for natural grunerite. The largest peak in the difference-Fourier synthesis for the natural sample has positional coordinates similar to those of Ca in calcic amphiboles. This peak was entered into the structure model as M4′ and was refined using scattering factors for Ca with the isotropic factor B fixed at 0.76, a value similar to that for Ca at M4 in tschermakitic hornblende (Phillips et al., 1989). This refinement yielded positional coordinates 0, 0.290(3), ½ and an M4′ occupancy that corresponds to a Ca content of 0.020(4) atoms per formula unit. Thus, the total number of electrons per formula unit at the M sites determined by site refinement is 169.3 for the natural grunerite, which is in relatively good agreement with the value 170.4 that was calculated from the chemical analysis of Clowe et al. (1988) using all of the nontetrahedral cations except H.

Although EDS analysis of the 2-h sample indicates that Ca remains in the grunerite phase during oxidation, the M4′ difference-Fourier peak observed in the natural sample is not present in any of the oxidized structures. Previous studies of air-heated amphiboles have shown that Na (Ungaretti, 1980; Phillips et al., 1989) and even Ca (Ungaretti, personal communication, 1987) may migrate from M4 to the A site during oxidation. Phillips et al. (1988, 1989) have suggested that this migration enables enhanced interaction between the A-site cation and the O3 anion that partially offsets the charge imbalance at O3 arising from dehydrogenation. It appears likely the small amount of Ca in this grunerite may have also migrated from M4′ to the A site during oxidation. No evidence for A-site occupancy in any oxidized structure was found in difference-Fourier syntheses; however, this absence may be due to the small concentration of Ca coupled with positional disorder at the A sites (see Hawthorne, 1983; Phillips et al., 1989).

The M-O bond lengths. The grand mean octahedral bond lengths [= (2 ⟨M1-O⟩ + 2 ⟨M2-O⟩ + ⟨M3-O⟩)/5] decrease from 2.125 (NAT) to 2.119 (30M), to 2.108 (2HR-A), and to 2.102 Å (2HR-B) in the grunerite crystals, reflecting the increase in Fe^{3+} content with oxidation. The maximum decrease in grand mean M-O bond length in this grunerite suite (0.017 or 0.023 Å) is greater than the 0.005 Å decrease observed in the tschermakitic hornblende (Phillips et al., 1989) but less than the 0.024 Å decrease reported for riebeckite (Ungaretti, 1980). These values suggest that the Fe^{3+} content of 2HR-A and 2HR-B structures is actually slightly less than for the air-heated riebeckite (Ungaretti, 1980), even though no partial decomposition was observed in the riebeckite.

Although smaller trivalent cations normally order at M2 in amphiboles, the mean octahedral bond length data indicate trivalent cations occupy both M1 and M3 in the oxidized amphiboles. With oxidation, ⟨M1-O⟩ shortens by 0.019, 0.071, and 0.036 or 0.024 Å in tschermakitic hornblende (Phillips et al., 1989), riebeckite (Ungaretti, 1980), and the grunerite samples, respectively. Likewise, decreases of 0.027, 0.063, and 0.004 or 0.007 Å are observed for ⟨M3-O⟩ in the respective structures.

The ⟨M2-O⟩ length also decreases (by 0.017 Å) with oxidation in grunerite. This contrasts with the increases reported for ⟨M2-O⟩ in both tschermakitic hornblende (0.021 Å) and riebeckite (0.043 Å). Phillips et al. (1988) have attributed the increases in ⟨M2-O⟩ in the hornblende and riebeckite to a partial reordering of existing trivalent cations from M2 to M1 and M3 during heating in order to alleviate partially the charge imbalance at O3 that arises from the dehydrogenation that accompanies oxidation. There are very few trivalent cations in natural grunerite, so there is no possibility of transferring trivalent cations from M2 during oxidation. Still, it is unclear why some Fe^{3+} produced during oxidation evidently resides at M2 rather than preferentially ordering at M1 and M3 as would be expected based on the behavior of the hornblende and riebeckite.

Discussion

Hodgson et al. (1965) reported that both dehydrogenation and oxygenation occurred in fibrous grunerite heated in air in the range 350–800 °C, although no decomposition was observed below 800 °C. In light of the present study, it now appears that the oxygenation process observed in grunerite by Hodgson et al. (1965) and subsequent investigators simply represents the initial stages of decomposition. Although these investigators were able to measure Fe^{2+} and OH contents with sufficient precision to determine that dehydrogenation was not the sole oxidation mechanism in grunerite, their heating experiments at lower temperatures evidently did not produce enough decomposition products to be detected by X-ray powder diffraction.

Hodgson et al. (1965) did find that the "oxy-grunerite" partially decomposes at around 800 °C to form pyroxene, spinel with an a cell edge only slightly less than that of magnetite, and hematite. Patterson and O'Connor (1966) also identified pyroxene and magnetite as decomposition products in a fibrous grunerite heated in air for 1 h at 950 °C. Ghose and Weidner (1971) conducted a series of heating experiments on grunerite in the 700–800 °C range under 500 bars Ar pressure. They found that under oxidizing conditions "oxy-grunerite" and traces of magnetite form, whereas under reducing conditions the grunerite

decomposed to form clinoferrosilite, amorphous silica, and H_2O.

The air-heated grunerite samples in the present study are also slightly magnetic, suggesting the presence of magnetite. As previously noted, SEM/EDS X-ray maps indicate the decomposition products are greatly enriched in Fe and largely depleted in Si and Mg relative to the grunerite, which is consistent with magnetite or hematite. Unfortunately, the small subhedral prismatic crystals such as those shown in Figure 1 were too small for reliable EDS analysis (R. Anderhalt, personal communication, 1989), so the presence or absence of a pyroxene phase could not be established.

It should be pointed out that any amphibole heated in air at these elevated temperatures is inherently unstable. Therefore, the products observed in an air-heated experiment may depend not only on factors such as temperature and duration of heating but also on the reaction kinetics. For example, it is possible to study oxidation effects in air-heated iron amphiboles only because the oxidation-dehydrogenation reaction occurs at a much faster rate than decomposition (Clowe et al., 1988). Because these reaction rates (especially those involving decomposition) may be strongly dependent on factors such as the type, number, and distribution of crystal imperfections, interpretations based on air-heated structures should be viewed with caution.

In this regard, it is interesting to note again that these air-heated grunerite samples apparently developed closely spaced incipient cleavage breaks, whereas tschermakitic hornblende (Phillips et al., 1989) and magnesio-hornblende (Phillips et al., in preparation) oxidized under similar conditions did not. Cleavage in amphiboles almost certainly involves breaking O bonds to M4, M2, and if present, A cations (Popp and Phillips, in preparation). Therefore, thermal expansion resulting from rapid heating might be more likely to induce cleavage in grunerite (which would promote decomposition) than in amphiboles with filled or partially filled A sites. Conversely, the initial stage of decomposition of air-heated grunerite, which apparently involves loss of Fe from M4 and M2, should facilitate cleavage development. By contrast, in air-heated alkali and calcic amphiboles, any Na (or Ca) lost from the M4 site during the early stages of oxidation migrates to the A site if vacancies are present (Ungaretti, 1980; Phillips et al., 1988, 1989).

The maximum extent of oxidation in these air-heated grunerite samples is greater than that induced in air-heated tschermakitic hornblende as gauged by changes in grand mean M-O bond lengths. However, it is less than that of the riebeckite air heated by Ungaretti (1980), in which no decomposition was observed. Furthermore, Ernst and Wai (1970) found that Fe-bearing sodic amphiboles heated in air at about 705 °C oxidized by dehydrogenation as long as H was present at O3. Therefore, it appears that the grunerite structure is less able to accommodate oxyamphibole components than are the alkali and, presumably, calcic amphiboles. This conclusion was also reached by Clowe et al. (1988) based on results from extensive hydrothermal experiments performed with various solid O buffers on a variety of natural Fe-bearing clinoamphiboles.

Thus, it appears that the key to the structural stability (or metastability) of Fe-rich clinoamphiboles under oxidizing conditions at elevated temperatures is the ability of the structure to compensate for the local charge imbalance arising at O3 from dehydrogenation (as described by Phillips et al., 1988, 1989). At least in air-heated samples, the ability of the A site to accommodate Na and Ca, but not Fe, lost from M4 during oxidation may also play a role.

Acknowledgments

Comments and suggestions by Tamsin McCormick and Jeff Swope led to improvements of the original manuscript. Bob Anderhalt, Philips Electronic Instruments, provided SEM photographs and EDAX analyses. This study was supported by NSF grants EAR-8312878 and EAR-8816257 to R.K.P. and EAR-8816650 to M.W.P. The X-Ray Diffraction Facility at the University of Toledo is maintained and operated by support from the College of Arts and Sciences.

References cited

Addison, W.E., and Sharp, J.H. (1968) Redox behavior of amosite. In Papers and Proceeding of the Fifth General Meeting of the International Mineralogical Association, Cambridge, 1966, p. 305–311. Mineralogical Society, London.

Barnes, V.E. (1930) Changes in hornblende at about 800 °C. American Mineralogist, 15, 393–417.

Bocchio, R., Ungaretti, L., and Rossi, G. (1978) Crystal-chemical study of eclogitic amphiboles from Alpe Arami, Lepontine Alps, southern Switzerland. Rendiconti Società Italiana Mineralogia et Petrologia, 34, 453–470.

Clowe, C.A., Popp, R.K., and Fritz, S.J. (1988) Experimental investigation of the relation between oxygen fugacity, ferric-ferrous ratio and unit cell parameters in four natural clinoamphiboles. American Mineralogist, 73, 487–499.

Ernst, W.G., and Wai, C.M. (1970) Mössbauer, infrared, X-ray and optical study of cation ordering and dehydrogenation in natural and heat-treated sodic amphiboles. American Mineralogist, 55, 1226–1258.

Finger, L.W. (1969) The crystal structure and cation distribution of a grunerite. Mineralogical Society of America, Special Paper no. 2, 95–100.

Frenz, B.A. (1978) The Enraf-Nonius CAD-4 SDP: A real time system for concurrent X-ray data collection and crystal structure solution. In H. Schenk, R. Olthof-Hazekamp, H. van Koningsueld, and G.C. Bassi, Eds., Computing in crystallography, p. 64–71. Delft University Press, Delft.

Fritz, S.J., and Popp, R.K. (1985) A single-dissolution technique for determining FeO and Fe_2O_3 in rock and mineral samples. American Mineralogist, 70, 961–968.

Ghose, S., and Weidner, J.R. (1971) Oriented transformation of grunerite to clinoferrosilite at 775 °C and 500 bars argon pressure. Contributions to Mineralogy and Petrology, 30, 64–71.

——— (1972) Mg^{2+}-Fe^{2+} order-disorder in cummingtonite, $(Mg,Fe)_7Si_8O_{22}(OH)_2$; a new geothermometer. Earth and Planetary Science Letters, 16, 346–354.

Hawthorne, F.C. (1983) The crystal chemistry of the amphiboles. Canadian Mineralogist, 21, 173–480.

Hodgson, A.A., Freeman, A.G., and Taylor, H.F.W. (1965) The thermal decomposition of amosite. Mineralogical Magazine, 35, 445–462.

Ibers, J.A., and Hamilton, W.C. (1964) Dispersion corrections and crystal structure refinements. Acta Crystallographica, 17, 781–782.

International tables for X-ray crystallography (1974) vol. 4. Kynoch Press, Birmingham, England.

Klein, C. (1964) Cummingtonite-grunerite series: A chemical, optical, and X-ray study. American Mineralogist, 49, 963–982.

North, A.C.T., Phillips, D.C., and Mathews, F.S. (1968) A semi-empirical method of adsorption correction. Acta Crystallographica, A24, 351–359.

Papike, J.J., and Ross, M. (1970) Gedrites: Crystal structures and intracrystalline cation distributions. American Mineralogist, 55, 1945–1972.

Patterson, J.H., and O'Connor, D.J. (1966) Chemical studies of amphibole asbestos: Structural changes of heat-treated crocidolite, amosite, and tremolite from infrared absorption studies. Australian Journal of Chemistry, 19, 1155–1164.

Phillips, M.W., Popp, R.K., and Clowe, C.A. (1988) Structural adjustments accompanying oxidation-dehydrogenation in amphiboles. American Mineralogist, 73, 500–506.

Phillips, M.W., Draheim, J.E., Popp, R.K., Clowe, C.A., and Pinkerton, A.A., (1989) Effects of oxidation-dehydrogenation in tschermakitic hornblende. American Mineralogist, 74, 764–773.

Rouxhet, P.G., Gillard, J.L., and Fripiat, J.J. (1972) Thermal decomposition of amosite, crocidolite, and biotite. Mineralogical Magazine, 38, 583–592.

Schurmann, K., and Hafner, S., (1971) Temperature dependent distribution of magnesium and iron in cummingtonites. Nature Physical Science, 231, 155–156.

Ungaretti, L. (1980) Recent developments in X-ray single crystal diffractometry applied to the crystal-chemical study of amphiboles. Godisnjak Jugoslavenskog Centra za Kristalografiju, 15, 29–65.

Walker, N., and Stuart, D. (1983) An empirical method for correcting diffractometer data for absorption effects. Acta Crystallographica, A39, 158–166.

Zachariasen, W.H. (1963) The secondary extinction correction. Acta Crystallographica, 16, 1139–1144.

——— (1967) A general theory of X-ray diffraction in crystals. Acta Crystallographica, 23, 558–564.

Manuscript received November 29, 1990
Manuscript accepted May 23, 1991